Kent Academic Repository

Integrated energy hub system based on power-to-gas and compressed air energy storage technologies in the presence of multiple shiftable loads

Mohammad Amin Mirzaei[1], Morteza Zare Oskouei[1], Behnam Mohammadi-Ivatloo[1,2] ✉, Abdolah Loni[3], Kazem Zare[1], Mousa Marzband[3], Mahmood Shafiee[4]

[1]*Smart Energy Systems Laboratory, Faculty of Electrical and Computer Engineering, University of Tabriz, Tabriz, Iran*
[2]*Institute of Research and Development, Duy Tan University, Da Nang 550000, Vietnam*
[3]*Department of Mechanical and Electrical Engineering, Northumbria University, Newcastle, UK*
[4]*School of Engineering and Digital Arts, University of Kent, Canterbury, UK*
✉ *E-mail: bmohammadi@tabrizu.ac.ir*

Q1
Q2
Abstract: Integrated energy carriers in the framework of energy hub system (EHS) have an undeniable role in reducing operating costs and increasing energy efficiency as well as system's reliability. Nowadays, power-to-gas (P2G), as a novel technology, is a great choice to intensify the interdependency between electricity and natural gas networks. The proposed strategy of this study is divided into three parts: (i) a stochastic model is presented to determine the optimal day-ahead scheduling of the EHS with the coordinated operating of P2G storage and tri-state compressed air energy storage (CAES) system. The main objective of the proposed strategy is to indicate the positive impact of P2G storage and tri-state CAES on lessening the uncertainty derived from renewable sources and the operating cost of EHS, including combined heat and power, heat storage system, gas boiler, and a wind turbine that would meet the demands of electrical, gas, and thermal. Also, the uncertainty of electricity market price, power generation of the wind turbine, and even electrical, gas, and thermal demands are considered. (ii) A demand response programme focusing on day-ahead load shifting is applied to the multiple electrical loads according to the load's activity schedule. (iii) The conditional value-at-risk algorithm, as a risk measure technique, is utilised with the proposed strategy to evaluate the risk-aversion of the EHS's operator. The proposed strategy is successfully applied to an illustrative example and is solved by general algebraic modelling system software. The obtained results validate the proposed strategy by demonstrating the considerable diminution in the operating cost of the EHS by almost 4.5%.

Nomenclature

Indices

b	gas boiler (GB)
c	charging mode
d	discharging mode
hs	heat storage
i	combined heat and power (CHP) unit
k	compressed air energy storage (CAES) system
m	active load
pg	power-to-gas (P2G) storage
s	scenario
si	simple cycle mode
t	time interval

Parameters

NT	total scheduling period
NI	total CHP units
NK	total CAES systems
NHS	total heat storage systems
NB	total GB units
NS	total scenarios
$\text{VOM}^{\text{Exp}}, \text{VOM}^C$	variable operation cost of expander/compressor of CAES system
$\lambda^e_{t,s}$	power price
$\lambda^g_{t,s}$	gas price
$A^{k,\max}, A^{k,\min}$	max/min energy capacity of CAES system
$B^{\text{hs},\max}, B^{\text{hs},\min}$	max/min capacity of heat storage

$B^{\text{hs},(\cdot),\max}$	maximum charge/discharge rate of heat storage
$\text{DL}_{t,s}$	electrical demand
$\text{DR}_{m,t,s}$	adjustable load value of active loads
$\text{GL}_{t,s}$	gas demand
$G^{\text{pg},(\cdot),\max}$	maximum stored/supplied gas by P2G storage
$\text{GT}^{B,\max}, \text{GT}^{S,\max}$	maximum exchanged gas energy
$H^{b,\max}, H^{b,\min}$	max/min capacity of GB
$\text{HL}_{t,s}$	heat demand
Inc_m	incentive cost of active shiftable loads
$P^{i,\max}, P^{i,\min}$	max/min generated power of CHP unit
$P^{k,c,\max}, P^{k,c,\min}$	max/min charge capacity of CAES system
$P^{k,d,\max}, P^{k,d,\min}$	max/min discharge capacity of CAES system
$P^{k,si,\max}, P^{k,si,\min}$	max/min capacity of CAES system in simple cycle mode
$P^{\text{pg},\max}$	maximum consumed power by P2G storage
$\text{PL}^{B,\max}, \text{PL}^{S,\max}$	maximum exchanged power
$R^{i,\text{up}}, R^{i,\text{dn}}$	up/down ramp rate limit of CHP unit
$\text{SU}^{(\cdot)}_{t,s}, \text{SD}^{(\cdot)}_{t,s}$	start-up and shut-down fuel consumption
$T^{i,\text{ON}}, T^{i,\text{OFF}}$	minimum on/off time interval of CHP unit
UT^i, DT^i	minimum up and down time of CHP unit
$V^{\text{pg},\max}, V^{\text{pg},\min}$	max/min capacity of P2G storage
$\eta^{\text{hs}}, \eta^{\text{hs},c}, \eta^{\text{hs},d}$	the efficiency of heat storage in standby/charge/discharge.
$\eta^{k,c}, \eta^{k,d}, \eta^{k,si}$	the efficiency of CAES system in charge/discharge/simple cycle mode
$\eta^i, \eta^b, \eta^{\text{pg}}$	the efficiency of CHP unit, GB, P2G storage
π_s	probability of scenarios
β	risk factor

Decision variables

$A_{t,s}^{k}$	energy level of CAES system
$B_{t,s}^{\mathrm{hs}}$	energy level of heat storage
$d_{t,s}^{\mathrm{DR}}$	electrical load after implementation of demand response programme (DRP)
$dr_{m,t,s}^{\mathrm{up}}, dr_{m,t,s}^{\mathrm{dn}}$	electrical load change after implementation of load shifting programme
$\mathrm{EL}_{t,s}^{+}, \mathrm{EL}_{t,s}^{-}$	bought/sold power from/to upstream power network
$G_{t,s}^{\mathrm{pg},c}$	gas stored by P2G storage
$G_{t,s}^{\mathrm{pg},d}$	gas supplied by P2G storage
$\mathrm{GE}_{t,s}^{\mathrm{pg}}$	gas produced by P2G storage
$\mathrm{GB}_{t,s}^{b}$	gas consumed by GB
$\mathrm{GC}_{t,s}^{i}$	gas consumed by CHP unit
$\mathrm{GK}_{t,s}^{k}$	gas consumed by CAES system
$\mathrm{GM}_{t,s}^{+}, \mathrm{GM}_{t,s}^{-}$	bought/sold gas from/to upstream gas network
$H_{t,s}^{i}$	generated heat by CHP unit
$H_{t,s}^{b}$	generated heat by GB
$H_{t,s}^{\mathrm{hs},d}$	heat supplied by heat storage
$H_{t,s}^{\mathrm{hs},c}$	heat stored by heat storage
$P_{t,s}^{i}$	generated power by CHP unit
$\mathrm{PW}_{t,s}$	generated wind power
$P_{t,s}^{\mathrm{pg}}$	power consumed by P2G storage
$P_{t,s}^{k,si}, P_{t,s}^{k,d}$	generated power in simple cycle/discharge mode by CAES system
$P_{t,s}^{k,c}$	consumed power in charge mode by CAES
$V_{t,s}^{\mathrm{pg}}$	energy level of P2G storage
M	positive constant
$I_{t,s}^{(\cdot)}, Y_{t,s}^{i}, Z_{t,s}^{i}$	binary variables to indicate the status of different equipment
$e_{t,s}^{(\cdot)}, g_{t,s}^{(\cdot)}$	binary variables to indicate bought/sold energy from/to upstream networks

1 Introduction

Nowadays, the use of natural gas as an alternative source for coal and nuclear fuels is an ideal solution to supply electrical demands in three energy sectors of residential, commercial, and industrial. Various technical methods have been developed to optimally integrate natural gas networks with the electricity grid and increase energy efficiency in electrical systems [1]. The main approach of these methods is to create a suitable platform based on different multi-stage optimisation programmes to optimise the energy flow in the integrated systems [2–4]. Establishing an appropriate connection between electricity and natural gas networks brings many benefits to the society (such as reducing the greenhouse gas emissions), consumers (such as decreasing energy price), and grid operators (such as boosting the power system reliability) [5–7]. For this reason, in recent years, the energy hub system (EHS) as an emerging concept has been utilised to supply the demands of electrical, thermal, and gas [8]. Conversion facilities and up-to-date energy storage technologies in the EHS have an important role to fulfil the various demands of consumers via creating an optimal connection between electricity and gas networks. To increase the efficiency and decrease the operating cost of the EHS, making the use of advanced technologies such as power-to-gas (P2G) storage and tri-state compressed air energy storage (CAES) system is essential [9–13]. The tri-state refers to three CAES modes including charge, discharge, and simple cycle. Utilising the CAES in the simple cycle mode in coordination with P2G enables more efficient exploitation of the gas network and improves the interdependencies between electricity and natural gas networks in the EHS. This combined operation scheme provides significant arbitrage opportunities by converting electrical energy into natural gas during low-electrical price hours. Also, it provides the electric power generation of the natural gas network at low-gas price hours [14]. Furthermore, the use of CAES in comparison with other

electrical storage systems has many advantages for the EHS's operator such as (i) storing a large amount of energy, (ii) unlike pumped hydroelectric storage, it does not need a specific location for installation, and (iii) agility-wise (quick response to possible changes in pressure times) [15].

As stated in the literature, the optimisation of EHS operation in the day-ahead market with consideration of different equipment has attracted much attention from the researchers' perspective. The optimisation frameworks have been modelled based on several different aspects of the EHS. The main objectives of the proposed structures are (i) reducing the total operating cost [16], (ii) increasing the penetration of renewable energy sources [17], (iii) supplying the various energy demands [18], (iv) applying different approaches to modelling the stochastic programming [19, 20], and (v) executing demand response programmes (DRPs) aiming at reducing the consumers' bill [21].

According to the above-mentioned aspects, numerous works have investigated the challenges associated with the EHS operation. Mainly, the shortcomings (*Sh*) of the existing literature are summarised as follows:

Sh1: The optimal scheduling of the EHS has been investigated in [22–24], considering the various equipment and different uncertainty methodologies. In these studies, the short-term EHS scheduling for multiple energy networks consisting of electricity and natural gas have been studied to reduce or compensate the uncertainty in the wind power generation and/or electrical demand. Furthermore, in [25, 26], the total system's cost minimisation in the multi-carrier energy systems has been followed up considering uncertainties regarding electrical demand and day-ahead electricity market prices. Nevertheless

(i) the effect of the P2G storage was not considered in the above-mentioned studies to determine the proper operation of the EHS, compensate the uncertainty in the output power of renewable resources, and decrease the day-ahead operating cost.
(ii) the benefits of tri-state CAES were ignored in the reviewed literature as the efficient storage device that has the potential to affect the operating cost of the EHS.
(iii) the uncertainties of electrical, gas, and thermal demands were not estimated in presented approaches in [25, 26], and
(iv) the impact of gas demand on the optimality of the results was not studied in [22, 23].

Sh2: DRPs have been implemented in [27–29] to meet the energy demands in the EHS. In these works, the main concern is to decrease the effect of various variable uncertainties associated with the distributed power generation systems and electrical demands on the optimal operation of the EHS by utilising DRPs. Also, time-based rate programmes as the major demand response techniques have been implemented in the electrical demands of the EHS to achieve the desired goals. However, the impact of customer satisfaction was not taken into account for DRPs in any of the aforementioned papers.

To tackle the mentioned issues, this study proposes a comprehensive EHS based on the P2G storage and tri-CAES system. Also, the conditional value-at-risk (CVaR) methodology is utilised to quantify the potential risk of the EHS scheduling problem. The proposed model schedules an integrated EHS considering combined heat and power (CHP) unit, heat storage system, gas boiler (GB) unit, and wind turbine in the presence of the load-shifting technique. The load activity schedule is utilised for the load-shifting programme according to customer satisfaction. Besides heating and electrical demands, gas demands are considered. For achieving more accurate results, the uncertainties derived from the electricity market price, power generation of the wind turbine, and electrical, gas, and thermal demands are estimated. In general, the main contributions (**C**) of this study can be listed as follows:

C1: Proposing integrated EHS with P2G storage and tri-CAES system to reduce the total operating cost of the EHS and
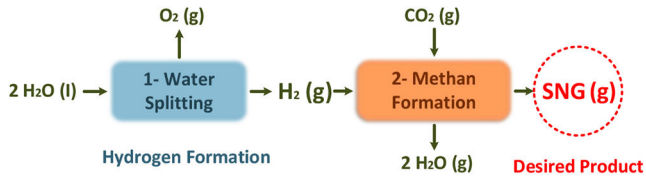
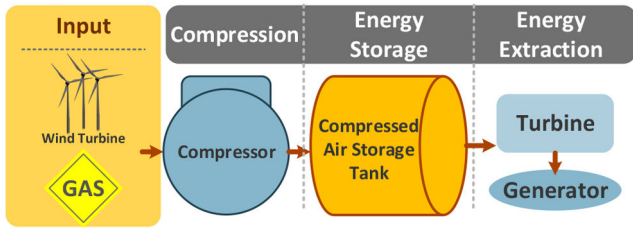**Fig. 1** *CH$_4$ formation mechanism by P2G pathway*

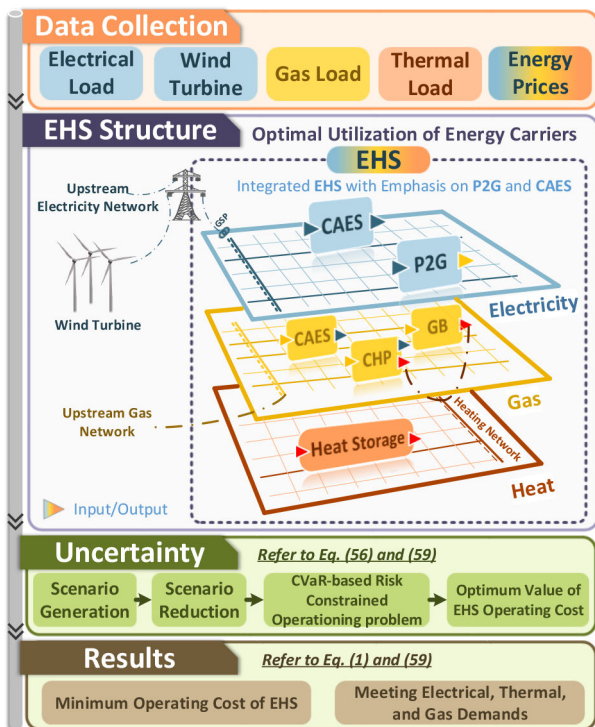**Fig. 2** *CAES process based on wind turbine generation*

Fig. 3 *Schematic for the integrated EHS*

compensate the uncertainty in the output power of wind turbine, electricity, heat and gas demands (*Tackled Sh1*).

C2: Implementing DRPs based on load shifting to reduce the operating cost of the EHS, considering the multiple electrical loads' activity schedule including residential, commercial, and industrial (*Tackled Sh2*).

The remaining parts of this paper are organised as follows: Section 2 presents the structure of the proposed model in this study. The mathematical formulation and constraints regarding the optimal scheduling of EHS are provided in Section 3. Section 4 presents simulation results and discussions on the obtained results. Finally, the conclusions are presented in Section 5.

2 Description of proposed framework

2.1 P2G concept

The P2G storage makes use of electricity to split water into hydrogen and oxygen via electrolysis, which can be described by $2H_2O \longrightarrow 2H_2 + O_2$. This emerging technology may be alkaline electrolysis or proton exchange membrane. The produced hydrogen interacts with carbon dioxide by means of Sabatier reaction, which

results in synthetic natural gas (SNG): $CO_2 + 4H_2 \longrightarrow CH_4 + 2H_2O$. This progress may be either chemical or biological. In Fig. 1, these two processes represent the major steps in developing the P2G technology. The overall energy conversion efficiency of a traditional P2G technology ranges between 50 and 60%. By increasing the energy conversion efficiency of P2G storage to 85%, P2G facilities can carry out cross-commodity arbitrage trade between electricity and natural gas markets aimed to lessen the operating cost of EHS [30]. When the price gap between electric energy and natural gas prices is remarkable to cover conversion losses, the EHS operator can profit from converting power to gas. Especially, the power to hydrogen (P2H) in the first stage is more efficient than the whole P2G process. Although, P2G storage offers several advantages over P2H, the utilisation of hydrogen is limited to fuel cells in certain industries. The produced SNG by P2G has more extensive applications and can be consumed by gas-fired units, which raises the operation flexibility of the two facilities. On the other hand, SNG has similar properties to conventional natural gas and thus can be stored, transmitted, and traded in the natural gas system. However, there are technical and legislative restrictions on the quantity of H$_2$ that may be injected into the natural gas network. Therefore, SNG is more realistic in prevailing conditions and P2G technology is considered in this study.

2.2 CAES concept

Nowadays, the use of CAES is becoming popular in comparison with other energy storage systems. The reason for this popularity is that the CAES does not require a specific geographic location for installation compared to a pumped storage plant. Therefore, it can be installed and used in an unrestricted electrical network. In addition, CAES has a lower investment cost compared to the pumped storage plants [31]. Against other energy storage technologies, CAES is more appropriate for producing and storing high-capacity power. On the other hand, CAES has a very high rate of flexibility. For instance, the 110 MW McIntosh Power Plant with a productive capacity of 134 MW and compressive strength of 110 MW can change from complete production to complete compression in < 5 min [32]. Another advantage of the CAES is that it works in three modes including charging, discharging, and simple cycle. Moreover, it can generate power exactly like a gas-fired power plant. This technology compresses air when the electricity price is low. Then, the compressed air is stored in a salty dome-shaped space. In times of high electricity prices, this system can make use of compressed air to generate electricity. Hence, there is no need for extra gas to compress air. Therefore, with regard to the features mentioned, CAES can be considered as an alternative option for the hub operator to reduce the operating cost of EHS. Fig. 2 depicts the procedure of energy generation by a simple type of CAES.

2.3 Structure of EHS

Fig. 3 shows the structure of the EHS consisting of a CHP unit, heat storage system, GB unit, and wind turbine in coordination with the P2G storage and tri-CAES system. In the first step, the data regarding electrical, gas, and heat loads, as well as energy prices are collected. Secondly, the hub operator in the form of EHS uses energy carriers including electricity, gas, and heat in order to reduce somehow the operating cost. In more detail, this system is fed by the upstream gas and electricity networks and wind turbines. The P2G storage, tri-CAES system, and CHP unit are the coupling points between the upstream gas and electricity networks. The optimum operating schedule of P2G storage in coordination with the tri-CAES system and other EHS equipment can help system's operator to consider the uncertainties resulting from the wind turbine generation, electricity market price, and energy demands. The outputs of EHS include meeting the demands of electrical, gas, and thermal in three sectors (residential, commercial, and industrial). In more detail, the electrical, heat, and gas demands are described in the following subsubsections.
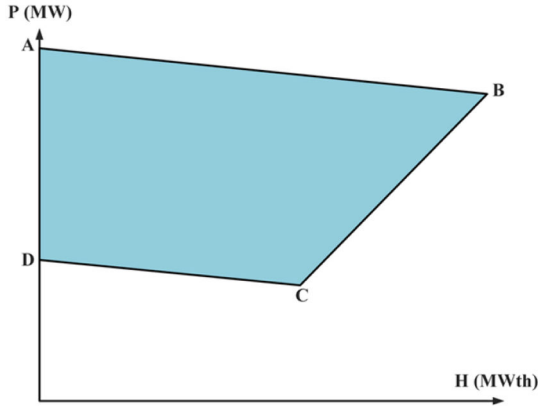
Fig. 4 *Feasible operating region of each CHP unit*

2.3.1 Electrical demand: As can be seen in Fig. 3, electrical demands are fulfilled by the upstream electricity network, wind turbines, CAES system, and CHP unit. The tri-state CAES system operates in one of the following three modes: (i) charging during low-price periods, (ii) discharging during high-price periods, and (iii) a simple cycle gas generator when the reservoir is evacuated or the gas and electricity prices are low and high, respectively. The simple cycle mode can present many economic opportunities for the hub system's operator.

2.3.2 Heat demand: Heat demand is fulfilled by the district heating network, heat storage system, CHP unit, and GB unit. Mainly, due to heat loss reduction, the district heating networks only meet the local demands of consumers in a local region. It should be pointed out that the converted energy could be utilised to store, for meeting gas demand, and as input fuel for CHP and GB units.

2.3.3 Gas demand: Gas demand is met by the upstream gas network and P2G storage. Some proportion of the purchased natural gas from the upstream gas network, as well as some of the power generated by P2G, is used to supply gas demand. In the time intervals when the electricity price is low, P2G storage could effectively convert electrical energy into compatible natural gas.

3 Problem formulation

In the day-ahead market, requests for the total hours of the next day are submitted to the day-ahead market at once. Day-ahead market prices for the total hours of the next day are determined at once when the day-ahead market is cleared, then the so-called second level uncertainty associated with the development of the real-time market takes place. Therefore, in this study, the EHS operator solves a day-ahead scheduling problem before submitting its bids to the day-ahead market in which the uncertainties related to the real-time stage are also modelled. Uncertainties associated with the real-time stage play an important role in sending the demand of the EHS to the energy market. In this section, a mathematical formulation is presented concerning the day-ahead scheduling of the EHS with the coordinated operating of the P2G storage and tri-state CAES system in the presence of load-shifting programme considering the technical constraints of the units. The stochastic objective function has been applied to minimise the total operating cost of the integrated EHS taking into account the uncertainties regarding electricity market price, time-varying generation of the wind turbine, and demands of electrical, gas, and heat. The objective function and constraints of the problem are explained in the following subsections.

3.1 Objective function

The objective function of the proposed model, as demonstrated in (1), aims at minimising total operating cost, which contains four mathematical expressions. The first term of the objective function determines the cost incurred and the revenue obtained from purchasing and selling electricity from/to the upstream electricity network. The electricity purchased from the upstream network is used to supply the hourly electrical demands and given as input to the P2G unit. The second term represents the variable operating and maintenance costs of the CAES unit in charging, discharging, and simple cycle modes. The third term of the objective function is associated with the natural gas purchased to support heat and gas demands, as well as the gas surplus sold to the upstream gas network. Given that the natural gas is utilised as the primary fuel for CHP, GB, and CAES units (in discharging and simple cycle modes), therefore, the operating costs of these units are considered in the third term of the objective function. Finally, the load-shifting programme cost is expressed in the fourth term. This term is related to the costs paid to the residential, commercial, and industrial consumers to execute the load-shifting programme

$$\min \sum_{s=1}^{NS} \pi_s \sum_{t=1}^{NT} \left[\begin{pmatrix} \lambda_{t,s}^e \mathrm{EL}_{t,s}^+ - \lambda_{t,s}^e \mathrm{EL}_{t,s}^- \\ + \sum_{k=1}^{NK} \begin{bmatrix} P_{t,s}^{k,d}\mathrm{VOM}^{\mathrm{Exp}} + \\ P_{t,s}^{k,si}(\mathrm{VOM}^{\mathrm{Exp}} + \mathrm{VOM}^C) \\ + P_{t,s}^{k,c}\mathrm{VOMC} \end{bmatrix} \\ + \lambda_{t,s}^g \mathrm{GM}_{t,s}^+ - \lambda_{t,s}^g \mathrm{GM}_{t,s}^- \\ + \sum_{m=1}^{NM} \mathrm{Inc}_m (dr_{m,t,s}^{\mathrm{dn}} + dr_{m,t,s}^{\mathrm{up}}) \end{pmatrix} \right] \qquad (1)$$

3.2 Problem constraints

3.2.1 CHP unit constraints: According to the nature of the co-generation units, the generation of heat and power affects the other generations. To illustrate this dependency, the heat-power feasible operating region of each CHP unit in the proposed integrated EHS is depicted in Fig. 4. To this end, linear equations are applied to describe the operating region of the CHP units, which are formulated by (2)–(6). In these equations, indices A, B, C, and D represent the marginal points of the feasible operating region for the CHP unit. Equations (2) and (3) ensure that the electricity and heat energy provided by the CHP unit do not exceed their permissible limits. Equation (4) models the area under the curve AB. Equations (5) and (6) model the upper area of curve BC and the upper area of curve CD, respectively

$$P^{i,\min} I_{t,s}^i \le P_{t,s}^i \le P^{i,\max} I_{t,s}^i \qquad (2)$$

$$0 \le H_{t,s}^i \le H_B^i \times I_{t,s}^i \qquad (3)$$

$$P_{t,s}^i - P_A^i - \frac{P_A^i - P_B^i}{H_A^i - H_B^i} \times (H_{t,s}^i - H_A^i) \le 0 \qquad (4)$$

$$P_{t,s}^i - P_B^i - \frac{P_B^i - P_C^i}{H_B^i - H_C^i} \cdot (H_{t,s}^i - H_B^i) \ge (I_{t,s}^i - 1) \cdot M \qquad (5)$$

$$P_{t,s}^i - P_C^i - \frac{P_C^i - P_D^i}{H_C^i - H_D^i} \cdot (H_{t,s}^i - H_C^i) \ge (I_{t,s}^i - 1) \cdot M \qquad (6)$$

The limitations of ramping up and down regarding the CHP unit are presented by (7)–(10), in which the binary variable is equal to one if each CHP unit is in the ON mode, otherwise it will be zero

$$P_{t,s}^i - P_{t-1,s}^i \le (1 - Y_{t,s}^i)R^{i,\mathrm{up}} + Y_{t,s}^i P^{i,\min} \qquad (7)$$

$$P_{t-1,s}^i - P_{t,s}^i \le (1 - Z_{t,s}^i)R^{i,\mathrm{dn}} + Z_{t,s}^i P^{i,\min} \qquad (8)$$

$$Y_{t,s}^i - Z_{t,s}^i = I_{t,s}^i - I_{t-1,s}^i \qquad (9)$$

$$Y_{t,s}^i + Z_{t,s}^i \ge 1 \qquad (10)$$

Equations (11)–(14) and (15)–(18) indicate the minimum up time and the minimum down time limits, respectively

$$\text{UT}^i = \max\left\{0,\ \min\left[\text{NT}, (T^{i,\text{ON}} - X^{i,\text{ON}}_{(t=0)})I^i_{(t=0)}\right]\right\} \quad (11)$$

$$\sum_{t=1}^{\text{UT}^i}(1 - I^i_{t,s}) = 0 \quad \forall t = 1, \dots, \text{UT}^i \quad (12)$$

$$\sum_{j=t}^{t+T^{i,\text{ON}}-1} I^i_{j,s} \geq T^{i,\text{ON}} Y^i_{t,s} \quad (13)$$

$$\forall t = \text{UT}^i + 1, \dots, \text{NT} - T^{i,\text{ON}} + 1$$

$$\sum_{j=t}^{\text{UT}^i}(I^i_{j,s} - Y^i_{t,s}) \geq 0 \qquad \forall t = \text{NT} - T^{i,\text{ON}} + 2, \dots, \text{NT} \quad (14)$$

$$\text{DT}^i = \max\left\{0,\ \min\left[\text{NT}, (T^{i,\text{OFF}} - X^{i,\text{OFF}}_{(t=0)})(1 - I^i_{(t=0)})\right]\right\} \quad (15)$$

$$\sum_{t=1}^{\text{DT}^i} I^i_{t,s} = 0 \quad \forall t = 1, \dots, \text{DT}^i \quad (16)$$

$$\sum_{j=t}^{t+T^{i,\text{OFF}}-1}(1 - I^i_{j,s}) \geq T^{i,\text{OFF}} Z^i_{t,s} \quad (17)$$

$$\forall t = \text{DT}^i + 1, \dots, \text{NT} - T^{i,\text{OFF}}$$

$$\sum_{j=t}^{\text{DT}^i}(1 - I^i_{j,s} - Z^i_{t,s}) \geq 0 \quad \forall t = \text{NT} - T^{i,\text{OFF}} + 2, \dots, \text{NT} \quad (18)$$

Start-up and shut-down fuel consumption of the CHP unit are calculated by (19) and (20) as follows:

$$\text{SU}^i_{t,s} \geq \text{sug}^i(I^i_{t,s} - I^i_{t-1,s})\ \text{SU}^i_{t,s} \geq 0 \quad (19)$$

$$\text{SD}^i_{t,s} \geq \text{sdg}^i(I^i_{t-1,s} - I^i_{t,s});\ \text{SD}^i_{t,s} \geq 0 \quad (20)$$

Equation (21) demonstrates the amount of natural gas consumed by the CHP unit

$$\text{GC}^i_{t,s} = \frac{P^i_{t,s}}{\eta^i} + \text{SU}^i_{t,s} + \text{SD}^i_{t,s} \quad (21)$$

3.2.2 GB constraints:
The upper and lower levels of the GB output for each scenario at any hour of the scheduling horizon are constrained by (22). In addition, the amount of natural gas consumed by GB with regard to its heat production at any hour is calculated by (23)

$$H^{b,\text{min}} \times I^b_{t,s} \leq H^b_{t,s} \leq H^{b,\text{max}} \times I^b_{t,s} \quad (22)$$

$$\text{GB}^b_{t,s} = \frac{H^b_{t,s}}{\eta^b} \quad (23)$$

3.2.3 Heat storage system constraints:
The reserved heat in the heat storage system for each scenario at any hour of the scheduling horizon is expressed by (24). Furthermore, (25) ensures that the thermal energy stored in the heat storage does not exceed the reservoir capacity. The ramping up/down rates of the heat storage are indicated by (26) and (27), respectively

$$B^{\text{hs}}_{t,s} = (1 - \eta^{\text{hs}})B^{\text{hs}}_{t-1,s} + H^{\text{hs},c}_{t,s} - H^{\text{hs},d}_{t,s}$$
$$- \beta_{\text{loss}}\text{SU}^{\text{hs}}_{t,s} + \beta_{\text{gain}}\text{SD}^{\text{hs}}_{t,s} \quad (24)$$

$$B^{\text{hs},\text{min}} \leq B^{\text{hs}}_{t,s} \leq B^{\text{hs},\text{max}} \quad (25)$$

$$B^{\text{hs}}_{t,s} - B^{\text{hs}}_{t-1,s} \leq B^{\text{hs},c,\text{max}} \quad (26)$$

$$B^{\text{hs}}_{t-1,s} - B^{\text{hs}}_{t,s} \leq B^{\text{hs},d,\text{max}} \quad (27)$$

3.2.4 CAES constraints:
Equation (28) prevents the CAES system to be operated simultaneously in three modes of charging, discharging, and simple cycle. The upper and lower levels of charging, discharging, and simple cycle modes of the CAES system are expressed by (29)–(31)

$$I^{k,c}_{t,s} + I^{k,d}_{t,s} + I^{k,si}_{t,s} \leq 1 \quad (28)$$

$$P^{k,c,\text{min}} I^{k,c}_{t,s} \leq P^{k,c}_{t,s} \leq P^{k,c,\text{max}} I^{k,c}_{t,s} \quad (29)$$

$$P^{k,d,\text{min}} I^{k,d}_{t,s} \leq P^{k,d}_{t,s} \leq P^{k,d,\text{max}} I^{k,d}_{t,s} \quad (30)$$

$$P^{k,si,\text{min}} I^{k,si}_{t,s} \leq P^{k,si}_{t,s} \leq P^{k,si,\text{max}} I^{k,si}_{t,s} \quad (31)$$

Equation (32) indicates that the reserved energy in the CAES in each hour depends on the energy levels in the previous time period, as well as charging and discharging energy. The range of the CAES reservoir is demonstrated by (33). Moreover, (34) states that the level of the CAES reservoir at the end of the scheduling must be equal to the initial level of the reservoir

$$A^k_{t,s} = A^k_{t-1,s} + \eta^{k,c}P^{k,c}_{t,s} - \frac{P^{k,d}_{t,s}}{\eta^{k,d}} \quad (32)$$

$$A^{k,\text{min}} \leq A^k_{t,s} \leq A^{k,\text{max}} \quad (33)$$

$$A^k_{0,s} = A^k_{\text{NT},s} \quad (34)$$

Equation (35) states the amount of natural gas consumed by CAES in discharging and simple cycle modes. It is worth mentioning that the CAES efficiency during discharge mode is twice the simple cycle mode [33].

$$\text{GK}^k_{t,s} = \frac{P^{k,d}_{t,s}}{\eta^{k,d}} + \frac{P^{k,si}_{t,s}}{\eta^{k,si}} \quad (35)$$

3.2.5 P2G storage constraints:
Converted natural gas by P2G storage can be injected into the upstream gas network or stored in the gas storage, as represented by (36). Also, the limit on electricity power consumed by the P2G storage is shown in (37)

$$G^{\text{pg},c}_{t,s} + \text{GE}^{\text{pg}}_{t,s} = \eta^{\text{pg}}P^{\text{pg}}_{t,s} \quad (36)$$

$$0 \leq P^{\text{pg}}_{t,s} \leq P^{\text{pg},\text{max}} \quad (37)$$

The reservoir balance, maximum capacity of injected and stored gas, and reservoir capacity limit of the P2G storage are specified by (38)–(42). Similar to other storage units, the gas reservoir level at the end of the scheduling period must be equal to the initial level of the reservoir, which is stated as (42)

$$V^{\text{pg}}_{t,s} = V^{\text{pg}}_{t-1,s} + G^{\text{pg},c}_{t,s} - G^{\text{pg},d}_{t,s} \quad (38)$$

$$0 \leq G^{\text{pg},c}_{t,s} \leq G^{\text{pg},c,\text{max}} \quad (39)$$

$$0 \leq G^{\text{pg},d}_{t,s} \leq G^{\text{pg},d,\text{max}} \quad (40)$$

$$V^{\text{pg},\text{min}} \leq V^{\text{pg}}_{t,s} \leq V^{\text{pg},\text{max}} \quad (41)$$

$$V^{\text{pg}}_{0,s} = V^{\text{pg}}_{\text{NT},s} \quad (42)$$

3.2.6 Upstream gas and electricity networks constraints:
The constraints of the electricity and natural gas exchange between the

integrated EHSs, the upstream gas and electricity networks are shown in (43)–(48). The binary variables are used to prevent the transmission and receipt of electricity and gas at the same time

$$0 \leq \mathrm{EL}_{t,s}^{+} \leq \mathrm{PL}^{B,\max} e_{t,s}^{+} \tag{43}$$

$$0 \leq \mathrm{EL}_{t,s}^{-} \leq \mathrm{PL}^{S,\max} e_{t,s}^{-} \tag{44}$$

$$e_{t,s}^{+} + e_{t,s}^{-} \leq 1 \tag{45}$$

$$0 \leq \mathrm{GM}_{t,s}^{+} \leq \mathrm{GT}^{B,\max} g_{t,s}^{+} \tag{46}$$

$$0 \leq \mathrm{GM}_{t,s}^{-} \leq \mathrm{GT}^{S,\max} g_{t,s}^{-} \tag{47}$$

$$g_{t,s}^{+} + g_{t,s}^{-} \leq 1 \tag{48}$$

3.2.7 Multiple load shifting constraints: The load-shifting programme is applied as one of the most effective methods of DSM technique to manage the electrical demands. Electrical demands consist of three components including residential, commercial, and industrial demands. To increase the customers' satisfaction, the load-shifting programme is utilised considering the multiple electrical loads' activity schedule. According to (49) and (50), the electrical demands of the EHS will be shifted from peak periods to the valley and off-peak periods concerning the participation rate of consumers and its activity schedule. Besides, the amount of variation in the first electrical load profile during the 24 h horizon should be equal to zero, which is shown in (51)

$$0 \leq dr_{m,t,s}^{\mathrm{up}} \leq \mathrm{DR}_{m,t} \times \mathrm{DL}_{t,s} \tag{49}$$

$$0 \leq dr_{m,t,s}^{\mathrm{dn}} \leq \mathrm{DR}_{m,t} \times \mathrm{DL}_{t,s} \tag{50}$$

$$\sum_{t=t_m}^{\mathrm{NT}_m} dr_{m,t,s}^{\mathrm{up}} = \sum_{t=t_m}^{\mathrm{NT}_m} dr_{m,t,s}^{\mathrm{dn}} \tag{51}$$

Eventually, the final demand profile of each sector is presented as follows:

$$d_{t,s}^{\mathrm{DR}} = \mathrm{DL}_{t,s} + dr_{m,t,s}^{\mathrm{up}} - dr_{m,t,s}^{\mathrm{dn}} \tag{52}$$

3.2.8 Multi-energy balance constraints: Equations (53)–(55) depict that each type of primary energy generated by the upstream networks plus the components of EHS must satisfy each type of demand, for each scenario at any hour of the scheduling horizon

$$\mathrm{EL}_{t,s}^{+} - \mathrm{EL}_{t,s}^{-} + \sum_{i=1}^{\mathrm{NI}} P_{t,s}^{i} + \mathrm{PW}_{t,s} - P_{t,s}^{\mathrm{pg}}$$
$$+ \sum_{k=1}^{\mathrm{NK}} (P_{t,s}^{k,si} + P_{t,s}^{k,d} - P_{t,s}^{k,c}) = d_{t,s}^{\mathrm{DR}} \tag{53}$$

$$\mathrm{GM}_{t,s}^{+} - \mathrm{GM}_{t,s}^{-} + \mathrm{GE}_{t,s}^{\mathrm{pg}} + G_{t,s}^{\mathrm{pg},d} - \sum_{i=1}^{\mathrm{NI}} \mathrm{GC}_{t,s}^{i}$$
$$- \sum_{k=1}^{\mathrm{NK}} \mathrm{GK}_{t,s}^{k} - \sum_{b=1}^{\mathrm{NB}} \mathrm{GB}_{t,s}^{b} = \mathrm{GL}_{t,s} \tag{54}$$

$$\sum_{i=1}^{\mathrm{NI}} H_{t,s}^{i} + \sum_{b=1}^{\mathrm{NB}} H_{t,s}^{b} + \sum_{h=1}^{\mathrm{NHS}} (H_{t,s}^{\mathrm{hs},d} - H_{t,s}^{\mathrm{hs},c}) = \mathrm{HL}_{t,s} \tag{55}$$

3.3 CVaR-based risk measurement

In this study, the risk of operating cost variability is modelled by the CVaR for a confidence level α. The CVaR is approximated by the operating cost of the $(1 - \alpha) \times 100\%$ scenarios with the highest

operating cost. The CVaR is calculated by solving the following optimisation problem:

$$\mathrm{CVaR} = \mathrm{Min}_{\mathrm{VaR}, \eta_s} \mathrm{VaR} + \frac{1}{1-a} \sum_{s=1}^{\mathrm{NS}} \pi_s \eta_s \tag{56}$$

$$\left[\sum_{t=1}^{\mathrm{NT}} \left(\begin{array}{l} \lambda_{t,s}^{e} \mathrm{EL}_{t,s}^{+} - \lambda_{t,s}^{e} \mathrm{EL}_{t,s}^{-} \\ + \sum_{k=1}^{\mathrm{NK}} \begin{bmatrix} P_{k,t,s}^{k,d} \mathrm{VOM}^{\mathrm{Exp}} + \\ P_{k,t,s}^{k,si} (\mathrm{VOM}^{\mathrm{exp}} + \mathrm{VOM}^{C}) \\ + P_{k,t,s}^{k,c} \mathrm{VOM}^{C} \end{bmatrix} \\ + \lambda_{t,s}^{g} \mathrm{GM}_{t,s}^{+} - \lambda_{t,s}^{g} \mathrm{GM}_{t,s}^{-} \\ + \sum_{m=1}^{\mathrm{NM}} \mathrm{Inc}_m dr_{m,t,s}^{\mathrm{dn}} + \sum_{m=1}^{\mathrm{NM}} \mathrm{Inc}_m dr_{m,t,s}^{\mathrm{up}} \end{array} \right) \right] - \mathrm{VaR} \leq \eta_s \tag{57}$$

$$\eta_s \geq 0 \tag{58}$$

For a given α in the open interval (0,1), VaR demonstrates the cheapest operating cost, as well as guaranteeing that the probability of achieving a total operating cost higher than the cheapest operating cost is lower than $(1 - \alpha)$. Besides, η_s is the difference between the operating cost in each scenario and VaR if the difference is positive; otherwise, it is equal to zero. Hence, considering CVaR-based risk, the problem is formulated as follows:

$$\min (1 - \beta) \sum_{s=1}^{\mathrm{NS}} \pi_s \sum_{t=1}^{\mathrm{NT}} \left(\begin{array}{l} \lambda_{t,s}^{e} \mathrm{EL}_{t,s}^{+} - \lambda_{t,s}^{e} \mathrm{EL}_{t,s}^{-} \\ + \sum_{k=1}^{\mathrm{NK}} \begin{bmatrix} P_{t,s}^{k,d} \mathrm{VOM}^{\mathrm{Exp}} + \\ P_{t,s}^{k,si} (\mathrm{VOM}^{\mathrm{Exp}} + \mathrm{VOM}^{C}) \\ + P_{t,s}^{k,c} \mathrm{VOM}^{C} \end{bmatrix} \\ + \lambda_{t,s}^{g} \mathrm{GM}_{t,s}^{+} - \lambda_{t,s}^{g} \mathrm{GM}_{t,s}^{-} \\ + \sum_{m=1}^{\mathrm{NM}} \mathrm{Inc}_m dr_{m,t,s}^{\mathrm{dn}} + \sum_{m=1}^{\mathrm{NM}} \mathrm{Inc}_m dr_{m,t,s}^{\mathrm{up}} \end{array} \right)$$
$$+ \beta \left(\varsigma + \frac{1}{1-a} \sum_{s=1}^{\mathrm{NS}} \pi_s \eta_s \right) \tag{59}$$

It should be pointed out that in this section, all constraints are similar to (2)–(52), as well as (57) and (58).

4 Results and discussion

The proposed model for the EHS in coordination with the P2G storage and CAES system is a mixed-integer programming. Computer simulations were performed by general algebraic modelling system (GAMS) software, CPLEX solver, running on a personal computer with a 2.4 GHz CPU with 6 GB of memory.

To evaluate the proposed model, the considered EHS includes a CHP, a GB, a wind farm, a heat storage system, a CAES, and a P2G storage system to supply the electrical, thermal, and gas loads. The parameters of the EHS are indicated in Tables 1–5. The load profile regarding electrical, thermal, gas, and wind farm is shown in Fig. 5. Also, the prices of the electricity market and natural gas are depicted in Fig. 6. The nominated wind farm capacity is 50 MW. The forecasted wind power is shown in Fig. 7. Monte–Carlo simulation has been applied to model the uncertainties associated with electrical, thermal, and gas loads, as well as wind turbine and electricity prices. It should be noted that electrical, thermal, and gas loads, as well as wind turbine and electricity prices, follow a normal distribution function with deviations of 5, 5, 5, 15, and 10%, respectively.

To evaluate the proposed model, the following four cases are considered:

4.1 Case 1: solving the problem with CAES and without considering uncertainty

In this case, the effect of the integration of the CAES system on EHS is investigated. Fig. 8 shows the hourly scheduling of the CAES system. As is shown, the hub operator purchases electricity from the upstream network/utility grid in times when the electricity prices are low and stores it in the CAES system as compressed air. Then, in times of high electricity prices, instead of purchasing power from the upstream network, the energy stored in the CAES

Table 1 Efficiency of the HUB

Parameter	Value
η^i	0.35
η^b	0.8
η^{hs}	0.9
η^{pg}	0.75
$\eta^{k,c}$	0.9
$\eta^{k,d}$	0.9
$\eta^{k,si}$	0.4

Table 2 Characteristics of CHP unit

Parameter	Value
$P^{i,\min}$, MW	48
$P^{i,\max}$, MW	105
$H^{i,\min}$, MWth	0
$H^{i,\max}$, MWth	87
initial status, h	1
min down, h	1
min up, h	1
ramp, MW/h	55

Table 3 Heat storage system parameters

Parameter, MWh	Value
$B^{hs,\min}$	0
$B^{hs,\max}$	60
$B^{hs,d,\max}$	20
$B^{hs,c,\max}$	20

Table 4 P2G storage system parameters

Parameter	Value
$V^{pg,\min}$, MWh	50
$V^{pg,\max}$, MWh	180
$G^{pg,d,\max}$, MW	40
$G^{pg,c,\max}$, MW	40
$P^{pg,\max}$, MW	50

Table 5 CAES system parameters

Parameter	Value
$A^{k,\min}$, MWh	50
$A^{k,\max}$, MWh	350
$P^{k,d,\min}$, MW	5
$P^{k,d,\max}$, MW	50
$P^{k,c,\min}$, MW	5
$P^{k,c,\max}$, MW	50
$P^{k,si,\min}$, MW	5
$P^{k,si,\max}$, MW	50

system is used to supply its consumption load. Also, since the CAES system has three active modes, the hub operator at hours 19, 20, and 21 when the electricity price is average, purchases power from the CAES system in the simple cycle mode. Fig. 9 depicts the impact of the CAES system on the power purchased from the upstream network in both non-CAES and CAES modes. As can be seen, during the hours when the CAES system is in charge, the amount of purchased power from the upstream network has increased and vice versa. In addition to this, Fig. 10 shows the effect of considering the CAES system on the gas purchased from the upstream network in two non-CAES and CAES modes. The amount of gas purchased from the upstream network has increased in the presence of the storage system, which increases the dependence of the EHS on natural gas. Table 6 indicates the impact of the CAES system on the total operating cost considering the CAES system with three active modes. As can be seen, while the purchased gas from the grid has increased, the purchasing power has decreased. It has led to a reduction in the total operating cost of hub EHS compared to non-CAES and CAES modes with two active modes (regardless of the simple cycle mode).

4.2 Case 2: case 1 with P2G system

In this case, the effect of integrating the P2G storage system into EHS in the presence of the CAES system is discussed. Fig. 11 explains how P2G is scheduled by the hub operator. In times of low electricity prices, the hub operator buys electricity from the upstream network and converts it into natural gas by P2G technology. The produced natural gas is stored in the storage system to be used when the gas price is high. It should be noted that the storage system in $t = 24$ is also in the charge mode due to the initial and final values of the energy stored in the gas storage should be equal. In the time intervals between 7–9 and 12–13, the hub operator makes use of gas stored in the storage system instead of purchasing natural gas from the upstream network to supply its gas loads. Fig. 12 states the impact of P2G storage on the gas and electricity purchased from the upstream network compared to case 1. As it can be seen, in the early hours when the storage is in charge, the power purchased from the upstream network has increased, and the amount of gas purchased from the upstream network has decreased during discharge mode. Table 7 indicates the effect of considering simultaneously the P2G storage and CAES system in the EHS. It has led to a reduction in the total amount of purchased gas and electricity, which confirms the advantages of taking into account these two technologies simultaneously in the EHS.

4.3 Case 3: case 2 with multiple loads

In this case, the impact of multiple shiftable loads on EHS is investigated. 10% of the load is considered as a shiftable, which includes 5% of industrial, 3% of commercial, and 2% of the residential loads. The active mode of each shiftable load is given in [34]. Fig. 13 shows the consequence of multiple shiftable loads on the electrical load profile of the energy hub. As it can be seen, in this case, loads of each industrial, commercial and residential sector, depending on their active mode, have shifted from the hours with high electricity prices to the hours with low electricity prices. It ultimately led to purchasing less amount of power by the hub operator in hours with high prices. Therefore, the operating cost of the EHS has dropped to $409,817.261 in comparison with case 2. Moreover, the effect of the participation rate of multiple shiftable loads on the operating cost of EHS is shown in Table 8. As can be seen, with increasing the participation coefficient of shiftable loads, the operating cost of EHS decreases, which is due to the decrease in purchasing electricity from the upstream network in high-cost hours.

4.4 Case 4: solving the risk-based stochastic problem by taking into account the uncertainties of cases 1–3

This case considers the uncertainty of EHS derived from electrical, gas, and thermal loads, electricity price, and the output power of the wind turbine. For this purpose, 1000 scenarios have been
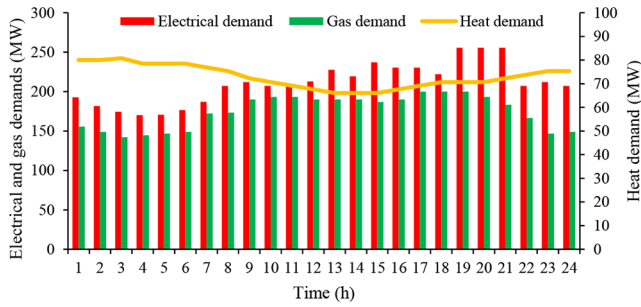
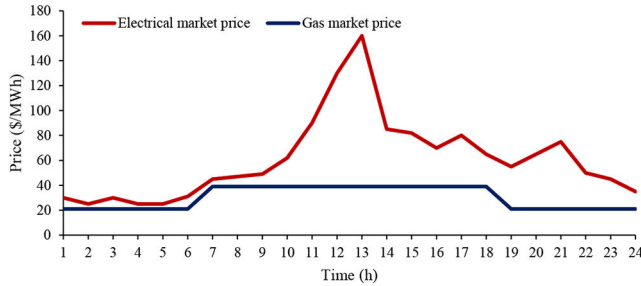**Fig. 5** *Predicted data for hourly electricity, heat and natural gas demands*

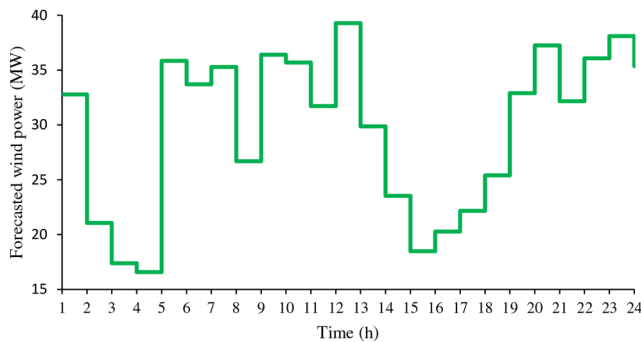
Fig. 6 *Predicted data for hourly prices of electricity and gas*
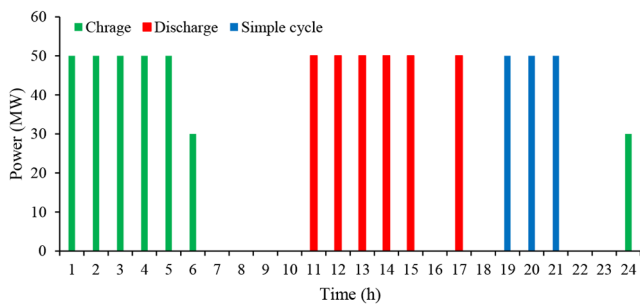

Fig. 7 *Forecasted wind power*
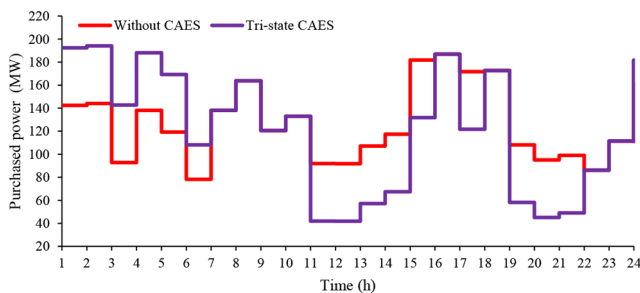

Fig. 8 *Hourly scheduling of CAES system*

Fig. 9 *The effect of CAES with three active modes on the electricity purchased from the electricity market*

Fig. 10 *The effect of CAES with three active modes on the gas purchased from the gas market*

Table 6 The effect of CAES on the operating cost of EHS

	Without CAES	With bi-state CAES	With tri-state CAES
gas operating cost, $	247,666.23	260,041.23	270,166.23
power operating cost, $	180,739.05	158,669.05	147819.05
total operating cost, $	428,405.27	418,710.27	417985.27
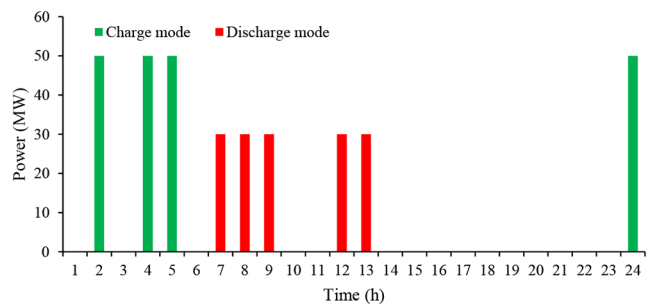
Fig. 11 *Hourly scheduling of P2G storage system*
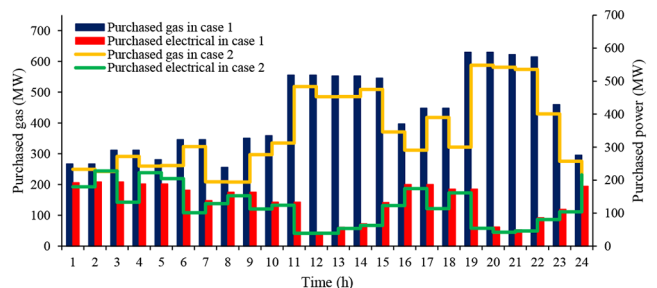
Fig. 12 *The effect of P2G on the power and gas purchased from the upstream network*

Table 7 The effect of P2G on the operating cost of EHS

	With tri-state CAES	Tri-state CAES +P2G storage
gas operating cost, $	270,166.227	264,316.227
power operating cost, $	147,819.048	152,619.047
total operating cost, $	417,985.274	416,935.274

Table 10 describes the expected operating cost under $\beta = 0$ for cases 1–3. It should be pointed out, in all three cases, the expected operating cost is higher than its predetermined value. Also, Table 11 states the effect of β variations on the operating cost of EHS, CVaR, and VAR for constant values of $\alpha = 0.9$. In this study, CVaR is defined as the expected operating cost in the top ten scenarios with the highest operating cost. As can be seen, when β has a direct relationship with the expected operating cost. In fact, higher operating costs occur at a lower risk level, and lower operating costs occur at a higher risk level. Hence, with an increase in β, the

generated using the Monte–Carlo simulation. Then, this number was reduced to ten scenarios by using the SCENRED GAMS tool. Table 9 shows the probability of occurrence for each scenario.
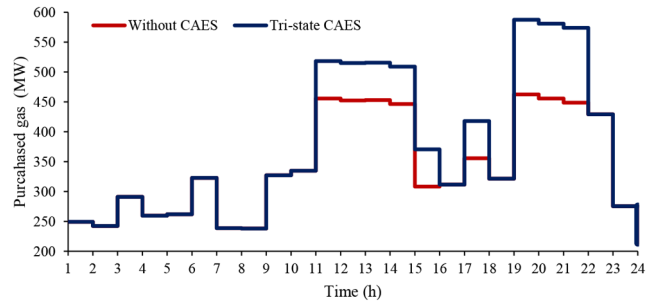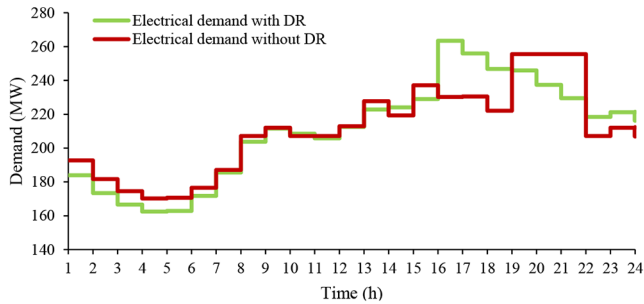
Fig. 13 *The effect of multiple shiftable loads on the EHS*

Table 8 The effect of the participation rate of multiple shiftable loads on the operating cost of EHS

Shiftable load, %	Total operating cost, $
10	409,817.26
12	408,169.04
14	406,520.83
16	404,872.61
18	403,253.43
20	401,814.37

Table 9 Probability of each scenario

Scenarios	Probability
S1	0.082
S2	0.132
S3	0.062
S4	0.188
S5	0.018
S6	0.205
S7	0.014
S8	0.078
S9	0.182
S10	0.039

Table 10 The expected operating cost of EHS considering the uncertainties of Case 1 to 3

	Case 1	Case 2	Case 3
expected gas operating cost, $	266,868.77	263,999.15	263,999.15
expected power operating cost, $	150,408.86	152,054.11	144,802.26
expected total operating cost, $	417,277.63	416,053.26	408,801.41

Table 11 The effect of increasing the beta coefficient on total operating cost, VaR, and CVaR

β	Total operating cost, $	VaR	CVaR
0.1	408,840.85	422,025.36	434,767.15
0.3	408,895.1	422,010.33	434,495.95
0.5	409,195.05	421,948.47	434,195.56
0.7	409,595.11	421,748.95	433,895.88
0.9	409,695.03	421,320.15	433,464.57

hub operator applies a more conservative strategy with lower risk levels, which leads to augmenting the operating cost of the energy hub. Furthermore, with the increase of β, due to applying a risk-averse approach, the expected operating cost in 10% of the scenarios having the highest operating cost will be reduced.

5 Conclusion

This study proposed a risk-constrained EHS integrated with the P2G storage and CAES systems in the presence of multiple shiftable loads. The Monte–Carlo simulation method was applied

to estimate the uncertainties concerning the electrical, thermal, and gas loads, wind turbine, and electricity prices. Also, the CVaR-based risk measurement was utilised to manage system uncertainties under a conservative approach. The results indicated that by increasing β, the hub operator would apply a more risk-averse strategy with a higher operating cost. The impacts of considering the P2G and CAES, and multiple shiftable loads can be summarised as follows:

(i) Taking into account the CAES storage in EHS has led to an increase and a decrease in the operating costs of gas and electricity, respectively. All in all, it reduces the operating cost of EHS. Considering this technology, along with its benefits, it will raise the dependence of EHS on the natural gas price.
(ii) Considering P2G technology, along with the CAES storage system, has led to a reduction in gas costs as well as the total operating cost of EHS. Therefore, it can compensate for the CAES system problem resulting from the increase in the natural gas costs.
(iii) Considering the multiple shiftable loads along with the P2G and CAES technologies have resulted in a reduction in the amount of electricity purchased from the upstream network. Hence, it has led to enhanced flexibility and dependency of EHS.

The work of this paper can be extended by focusing on regional-district co-optimisation of integrated power, gas, and heating systems. In addition, the constraints of the natural gas networks at the transmission level and district heating system can be considered in more detail. On the other hand, integrated demand response as a novel concept of DRPs is important to be researched for coordinated energy systems.

6 References

[1] Xu, Y., Ding, T., Ming, Q*., et al.*: 'Adaptive dynamic programming based gas-power network constrained unit commitment to accommodate renewable energy with combined-cycle units', *IEEE Trans. Sustain. Energy*, Early Access

[2] Ding, T., Hu, Y., Bie, Z.: 'Multi-stage stochastic programming with nonanticipativity constraints for expansion of combined power and natural gas systems', *IEEE Trans. Power Syst.*, 2018, **33**, (1), pp. 317–328

[3] Ding, T., Xu, Y., Yang, Y*., et al.*: 'A tight linear program for feasibility check and solutions to natural gas flow equations', *IEEE Trans. Power Syst.*, 2019, **34**, (3), pp. 2441–2444

[4] Ding, T., Xu, Y., Wei, W*., et al.*: 'Energy flow optimization for integrated power-gas generation and transmission systems', *IEEE Trans. Ind. Inf.*, 2020, **16**, (3), pp. 1677–1687

[5] Ghanaee, R., Akbari Foroud, A.: 'Economic analysis and optimal capacity sizing of turbo-expander-based microgrid', *IET Renew. Power Gener.*, 2017, **11**, (4), pp. 511–520

[6] Wang, C., Wei, W., Wang, J*., et al.*: 'Equilibrium of interdependent gas and electricity markets with marginal price based bilateral energy trading', *IEEE Trans. Power Syst.*, 2018, **33**, (5), pp. 4854–4867

[7] Mirzaei, M.A., Sadeghi-Yazdankhah, A., Mohammadi-Ivatloo, B*., et al.*: 'Integration of emerging resources in IGDT-based robust scheduling of combined power and natural gas systems considering flexible ramping products', *Energy*, 2019, **189**, p. 116195

[8] Vogelin, P., Georges, G., Boulouchos, K.: 'Design analysis of gas engine combined heat and power plants (CHP) for building and industry heat demand under varying price structures', *Energy*, 2017, **125**, pp. 356–366

[9] Nazari-Heris, M., Mirzaei, M.A., Mohammadi-Ivatloo, B*., et al.*: 'Economic-environmental effect of power to gas technology in coupled electricity and gas systems with price-responsive shiftable loads', *J. Clean. Prod.*, 2020, **244**, p. 118769

[10] Jadidbonab, M., Mousavi-Sarabi, H., Mohammadi-Ivatloo, B.: 'Risk-constrained scheduling of solar-based three state compressed air energy storage with waste thermal recovery unit in the thermal energy market environment', *IET Renew. Power Gener.*, 2019, **13**, (6), pp. 920–929

[11] Chen, S., Wei, Z., Sun, G*., et al.*: 'Steady state and transient simulation for electricity-gas integrated energy systems by using convex optimisation', *IET Gener. Transm. Distrib.*, 2018, **12**, (9), pp. 2199–2206

[12] Clegg, S., Mancarella, P.: 'Storing renewables in the gas network: modelling of power-to-gas seasonal storage flexibility in low carbon power systems', *IET Gener. Transm. Distrib.*, 2016, **10**, (3), pp. 566–575

[13] Zeng, Z., Ding, T., Xu, Y*., et al.*: 'Reliability evaluation for integrated power-gas systems with power-to-gas and gas storages', *IEEE Trans. Power Syst.*, 2020, **35**, (1), pp. 571–583

[14] Shams, M., Shahabi, M., Khodayar, M.: 'Stochastic day-ahead scheduling of multiple energy carrier microgrids with demand response', *Energy*, 2018, **155**, pp. 326–338

[15] Aliasghari, P., Zamani-Gargari, M., Mohammadi-Ivatloo, B.: 'Look-ahead risk-constrained scheduling of wind power integrated system with compressed air energy storage (CAES) plant', *Energy*, 2018, **160**, pp. 668–677

Q5 [2]

[16] Jadidbonab, M., Dolatabadi, A., Mohammadi-Ivatloo, B*., et al.*: 'Risk-constrained energy management of PV integrated smart energy hub in the presence of demand response program and compressed air energy', *IET Renew. Power Gener.*, 2019, **13**, (6), pp. 998–1008

[17] Pazouki, S., Haghifam, M.R.: 'Optimal planning and scheduling of energy hub in presence of wind, storage and demand response under uncertainty', *Electr. Power Energy Syst.*, 2016, **80**, pp. 219–239

[18] Massrur, H.R., Niknam, T., Fotuhi-Firuzabad, M.: 'Investigation of carrier demand response uncertainty on energy flow of renewable-based integrated electricity-gas-heat systems', *IEEE Trans. Ind. Inf.*, 2018, **14**, (11), pp. 5133–5142

[19] Gerami Moghaddam, I., Saniei, M., Mashhour, E.: 'A comprehensive model for self-scheduling an energy hub to supply cooling, heating and electrical demands of a building', *Energy*, 2016, **94**, pp. 157–170

[20] Alipour, M., Zare, K., Abapour, M.: 'MINLP probabilistic scheduling model for demand response programs integrated energy hubs', *IEEE Trans. Ind. Inf.*, 2018, **14**, (1), pp. 79–88

[21] Majidi, M., Nojavan, S., Zare, K.: 'A cost-emission framework for hub energy system under demand response program', *Energy*, 2017, **134**, pp. 157–166

[22] Huo, D., Le Blond, S., Gu, C*., et al.*: 'Optimal operation of interconnected energy hubs by using decomposed hybrid particle swarm and interior-point approach', *Int. J. Electr. Power Energy Syst.*, 2018, **95**, pp. 36–46

[23] Dolatabadi, A., Mohammadi-ivatloo, B., Abapour, M*., et al.*: 'Optimal stochastic design of wind integrated energy hub', *IEEE Trans. Ind. Inf.*, 2017, **13**, (5), pp. 2379–2388

[24] Dolatabadi, A., Jadidbonab, M., Mohammadi-Ivatloo, B.: 'Short-term scheduling strategy for wind-based energy hub: a hybrid stochastic/IGDT approach', *IEEE Trans. Sustain. Energy*, 2019, **10**, (1), pp. 438–448

[25] Ma, T., Wu, J., Hao, L.: 'Energy flow modeling and optimal operation analysis of the micro energy grid based on energy hub', *Energy Convers. Manage.*, 2017, **133**, pp. 292–306

[26] Roldan-Blay, C., Escriva, G.E., Roldan-Porta, C*., et al.*: 'An optimisation algorithm for distributed energy resources management in micro-scale energy hubs', *Energy*, 2017, **132**, pp. 126–135

[27] Vahid-Pakdel, M.J., Nojavan, S., Mohammadi-Ivatloo, B*., et al.*: 'Stochastic optimization of energy hub operation with consideration of thermal energy market and demand response', *Energy Convers. Manage.*, 2017, **145**, pp. 117–128

[28] Dolatabadi, A., Mohammadi-Ivatloo, B.: 'Stochastic risk-constrained scheduling of smart energy hub in the presence of wind power and demand response', *Appl. Therm. Eng.*, 2017, **123**, pp. 40–49

[29] Pazouki, S., Haghifam, M.R., Moser, A.: 'Uncertainty modeling in optimal operation of energy hub in presence of wind, storage and demand response', *Int. J. Electr. Power Energy Syst.*, 2014, **61**, pp. 335–345

[30] HELMETH: Integrated High-Temperature ELectrolysis and METHanation for Effective Power to Gas Conversion. Available at: http://www.helmeth.eu/index.php/project (accessed 10 July 2019)

[31] Soltani, Z., Ghaljehei, G.B., Gharehpetian, M*., et al.*: 'Integration of smart grid technologies in stochastic multi-objective unit commitment: an economic emission analysis', *Int. J. Electr. Power Energy Syst.*, 2018, **100**, pp. 565–590

[32] Mirzaei, M.A., Sadeghi Yazdankhah, A., Mohammadi-Ivatloo, B*., et al.*: 'Stochastic network-constrained co-optimization of energy and reserve products in renewable energy integrated power and gas networks with energy storage system', *J. Clean. Prod.*, 2019, **223**, pp. 747–758

[33] Safaei, H., Keith, D.W.: 'Compressed air energy storage with waste heat export: an alberta case study', *Energy Convers. Manage.*, 2014, **78**, pp. 114–124

[34] Zare Oskouei, M., Sadeghi Yazdankhah, A.: 'The role of coordinated load shifting and frequency-based pricing strategies in maximizing hybrid system profit', *Energy*, 2017, **135**, pp. 370–381

IET-GTD20191163

Author Queries

Q   Please make sure the supplied images are correct for both online (colour) and print (black and white). If changes are required please supply corrected source files along with any other corrections needed for the paper.

Q   All equations too long to fit within a single column are automatically floated to the bottom of the page and a '(see equation below)' or '(see (equation number) and (equation number)' left in their place. This is done automatically by our new XML transform, so please specify in your corrections very clearly where they should be broken as your paper is edited by non-experts.

Q1   Please confirm the changes made in the article title. Please note that it is the IET's house style to remove words such as "Novel", "New" and "Study of' from anywhere in the title if it makes sense to do so as well as "A", "An", "On the", and "The" from the beginning of the title unless the result makes no sense.

Q2   Please reduce the number of words in the Abstract to 200 words.

Q3   Please check the edits made to the sentence "Although, P2G storage offers...".

Q4   Please provide the expansion of the abbreviation [DSM]

Q5   Please provide year of publication, volume number and page range in Ref. [1].